Analytical study on lateral torsional buckling of partially encased beams under ISO834 fire exposure

Ana Belén Ramos-Gavilán,[1]
Paulo Piloto,[2] Luís Mesquita[3]

[1]University of Salamanca, Spain;
[2]Associated Laboratory for Energy, Transports and Aeronautics (LAETA-INEGI), Polytechnic Institute of Bragança; [3]Institute for Sustainability and Innovation in Structural Engineering, Polytechnic Institute of Bragança, Portugal

Abstract

European standard EN1994-1-2:2005 provides tabulated values and simplified calculation models for assessing fire resistance of composite beams, but does not consider the design checks against lateral torsional buckling under fire. This research presents an analytical method to calculate the buckling resistance moment of laterally unrestrained partially encased beams in fire conditions. The proposal applies a reduction factor for lateral torsional buckling in fire design condition to the moment resistance of the homogenised section at time *t*, determined by EN1994-1-2:2005. Two finite element models capable to simulate the thermal and mechanical behaviour of partially encased beams are also presented, including the validation against fire tests conducted by Piloto *et al*. Based on these models, a numerical analysis of partially encased beams with the same geometry and material properties as used in experimental tests is presented, evaluating different load levels when exposed to standard fire ISO834:1999. The numerical results of fire resistance according to standard EN1363-1:2012 and the numerical ultimate time, when beams suffer instability, are used to validate the proposal, using experimental and analytical heating result according to EN1994-1-2:2005.

Introduction

Partially encased beams (PEBs) are composite elements normally used to increase the massivity of I and H steel profiles by filling with concrete the spaces between flanges. This solution increases fire resistance, load bearing, and torsional and bending stiffness and, therefore, lateral

torsional buckling (LTB) resistance.

Lateral instability of PEBs at room temperature was experimentally investigated by Lindner and Budassis.[1] This research proposed a design LTB moment resistance taking into account the concrete torsional stiffness.

Maquoi *et al*.[2] developed an experimental and numerical study that improved the knowledge of LTB of PEBs. The elastic moment and the ultimate LTB moment were revised.

Kodaira *et al*.[3] determined the fire resistance of PEBs with and without concrete slabs. The study demonstrated that the reinforcement of concrete is effective during fire. The numerical analysis did not predict well the experimental thermal measurement, even the global thermo-mechanical behaviour adjusted to the experimental one.

Fire resistance in time domain of PEBs were experimentally investigated by Piloto *et al*.[4] The specimens were made of IPE100 steel 275JR section and C20/25 concrete with siliceous aggregates. The three-point bending tests were developed in vertical position inside a fire resistance furnace 1m length, as shown in Figure 1. The top support was a simple fork, the bottom one was built with a shaft inserted into drilled web, and the load was applied in all the flange depth at mid-span. The distance between supports was 1210 mm, studying three different load levels. Deflections and temperature measurements were determined under ISO834[5] fire exposure.

Standard EN1994-1-1:2004[6] provides certain design and calculation criteria for PEBs under bending at room temperature, including verification of LTB according to the procedure set out in standard EN1993-1-1:2005.[7] For its part, standard EN1994-1-2:2005[8] provides tabulated values and simplified calculation models for assessing the fire resistance (FR) of composite beams. These methods relate FR to load level, profile geometry and concrete reinforcement area, which compensates for the loss of resistance of the profile bottom flange. However, this standard does not take into account the design checks against LTB of laterally unrestrained PEBs under fire.

This research presents a new proposal to determine the buckling resistance moment of laterally unrestrained PEBs under fire, adapting the formulation of standard EN1993-1-2:2005[9] to PEBs. The analytical results are validated by a numerical study based on a three-dimensional FEM that simulates the behaviour of the PEBs analysed in the study conducted by Piloto *et al*.[4] The numerical analysis provides the time in which PEBs loss stability and the FR according to standard EN1363-1:2012,[10]

employing different load level under fire conditions. The numerical validation of the performed fire tests[4] are also included in this study, by temperature and displacement comparisons.

Materials and Methods

Lateral torsional buckling resistance of partially encased beams under fire conditions

The proposal to determine the buckling resistance moment of a laterally unrestrained PEBs under fire at time *t*, $M_{b,fi,t,Rd}$, consists of adapting the formulation of standard EN1993-1-2:2005[9] to PEBs, by using expression (1), where $\chi_{LT,fi}$ is the reduction factor for lateral torsional buckling in the fire design condition and $M_{fi,t,Rd}$ is the moment resistance of the homogenised section in the fire condition at time *t*.

$$M_{b,fi,t,Rd} = \chi_{LT,fi} \cdot M_{fi,t,Rd} \qquad (1)$$

The moment resistance of the homogenised partially encased section in the fire situation at time *t* is determined by the procedure set out in standard EN1994-1-2:2005,[8] establishing axial equilibrium, as shown in Figure 2, based on expression (2), where *b* and *h* are the profile dimensions, t_f and t_w are the thickness of the flange and web of the steel section, z_s and y_s represent the relative position for reinforcement, A_s is the effective area of longitudinal reinforcement, $f_{ay,w,t}$ is the strength of the web steel of the structural steel at time *t*, $f_{ay,f,t}$ is the strength of the flange steel of the structural steel at time t, $f_{c,t}$ is the strength of the concrete at time *t* and $z_{pl,fi,t}$ is the depth of the

plastic neutral axis at time t, determined by equation (3).

$$M_{fi,t,Rd} = W_{pl,fi} f_{ay,w,t} - 2 \cdot \left[t_w \left(\frac{h}{2} - z_{pl,fi,t} \right)^2 \frac{1}{2} f_{ay,w,t} \right] + 2A_s f_{sy,t} \cdot \left(\frac{h}{2} - z_s \right)$$
$$+ \left(z_{pl,fi,t} - t_f \right) \cdot (b - t_w) \cdot f_{c,t} \left(\frac{h}{2} - t_f - \frac{z_{pl,fi,t} - t_f}{2} \right) + \left(f_{ay,f,t} - f_{ay,w,t} \right) b t_f \left(h - t_f \right) \quad (2)$$

$$z_{pl,fi,t} = \frac{t_w f_{ay,w,t} h + (b - t_w) \cdot t_f \cdot f_{c,t}}{2 \cdot t_w f_{ay,w,t} + (b - t_w) \cdot f_{c,t}} \quad (3)$$

For steel beams, standard EN1993-1-2:2005[9] establishes that coefficient $\chi_{LT,fi}$ depends on the non-dimensional slenderness for lateral torsional buckling at the temperature of the compression flange of the section, $\lambda_{LT,q,com}$, and on the imperfection factor a, as shown by expressions (4), (5) and (6). The proposal to determine $l_{LT,q,com}$ in the case of PEBs is to use expression (7), where $M_{fi,t,Rk}$ is the moment resistance of the composite section at time t and $M_{cr,fi,t}$ represents the elastic critical moment at time t. The latter is obtained from the homogenised section, using the web steel modulus of elasticity and the shear modulus at time t, considering the flexural stiffness in the minor axis and 10% of the torsional stiffness of the complete encasement, and neglecting the concrete in the warping inertia of the homogeneous section, according to standard EN1994-1-1:2004.[6] 100% of concrete the torsional stiffness is also considered.

$$\chi_{LT,fi} = \frac{1}{\phi_{LT,\theta,com} + \sqrt{\left[\phi_{LT,\theta,com} \right]^2 - \left[\bar{\lambda}_{LT,\theta,com} \right]^2}} \quad (4)$$

$$\phi_{LT,\theta,com} = \frac{1}{2} \left[1 + \alpha \cdot \bar{\lambda}_{LT,\theta,com} + \left(\bar{\lambda}_{LT,\theta,com} \right)^2 \right] \quad (5)$$

$$\alpha = 0{,}65 \sqrt{\frac{235}{f_y}} \quad (6)$$

$$\bar{\lambda}_{LT,\theta,com} = \sqrt{\frac{M_{fi,t,Rk}}{M_{cr,fi,t}}} \quad (7)$$

Finally, based on the proposal of Vila Real *et al.*,[11] the reduction factor for lateral buckling is modified to take into account the variation in the bending moment diagram, depending on expressions (8) and (9), taking the k_c values specified by standard EN1993-1-1:2005[7].

$$\chi_{LT,fi,mod} = \frac{\chi_{LT,fi}}{f} \leq 1 \quad (8)$$

$$f = 1 - 0{,}5 \cdot (1 - k_c) \quad (9)$$

Heating of partially encased beams under fire conditions

Temperature evolution in PEBs under standard fire exposure[5] is determined according to standard EN1994-1-2:2005.[8] Two heating diagrams are proposed for this purpose: the first one considers different temperature evolution in flanges and web, assuming no heat transfer between them; the second one considers uniform section temperature, assuming that the heating of the web takes place through thermal conduction from the flanges, which are exposed to fire. In both cases, the formula for deter-
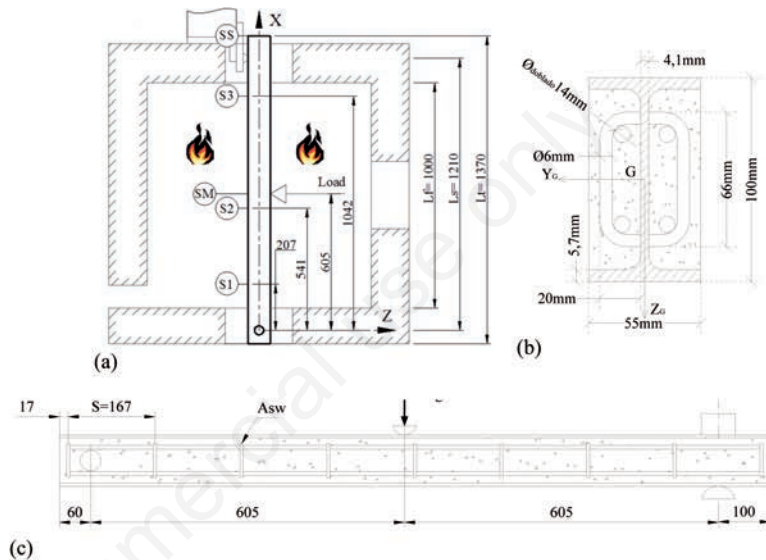

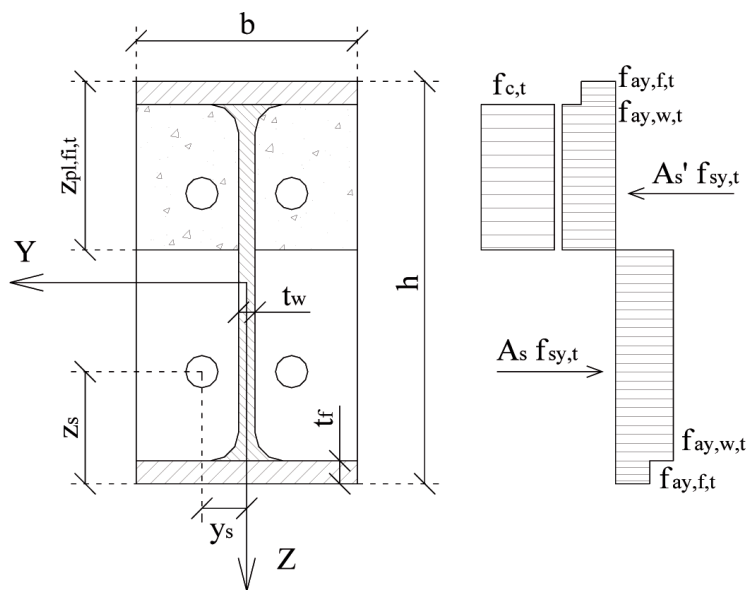**Figure 1. Trial diagram and description of the experimental test specimens.**

Figure 2. Stress distribution in partially encased beams for the calculation of moment resistance $M_{fi,t,Rd}$.

mining the heating range in unprotected steel members is used, expression (10), with the exception of the web when there is separation by components, where heating is determined through the expression used for protected steel, equations (11) and (12), assuming that the thermal properties of the concrete remain constant. In this expressions k_{sh} is the correction factor for the shadow effect, c_a is the specific heat of steel, ρ_a is the unit mass of steel, (A_i/V_i) is the section factors, c_p is the specific heat of the fire protection material, ρ_p is the unit mass of fire protection material, λ_p is the

thermal conductivity of the fire protection material, d_p is the thickness for fire protection material, $\Delta\theta_{g,t}$ is the increase of the ambient gas temperature during the time interval Δt, and h_{net} is the heat flux per unit area. Table 1 shows the section factors used in each of the calculation proposals.

$$\Delta\theta_{unf,t} / \Delta\theta_{f,t} = k_{sh}\left(\frac{1}{c_a \cdot \rho_a}\right) \cdot \left(\frac{A_i}{V_i}\right) \cdot \dot{h}_{net} \cdot \Delta t \qquad (10)$$

$$\Delta\theta_{w,t} = \left[\left(\frac{\lambda_p / d_p}{c_a \rho_a}\right) \cdot \left(\frac{A_{p,i}}{V_i}\right) \cdot \left(\frac{1}{1+w/3}\right)\right.$$
$$\left. \cdot (\theta_t - \theta_{w,t}) \cdot \Delta t \right] - \left[\left(e^{w/10} - 1\right) \cdot \Delta\theta_{g,t}\right] \qquad (11)$$

$$w = \left(\frac{c_p \rho_p}{c_a \rho_a}\right) \cdot d_p \cdot \left(\frac{A_{p,i}}{V_i}\right) \qquad (12)$$

To analyze the heating of the section under consideration, shown in Figure 1b, the temperature is assumed to be uniform in the section due to its reduced dimensions: beam depth does not exceed 500 mm. The net heat flux to the exposed surfaces considers heat transfer by convection and radiation, and is determined by using the coefficient of heat transfer by convection, α_c, by the gas temperature near the fire exposed member, q_g, at the temperature of the member surface, q_m, by the configuration factor, F, at the surface emissivity of the member, e_m, by the emissivity of the fire, e_f, and by the effective radiation temperature, qr, using expressions (13) (14) and (15).

$$\dot{h}_{net} = \dot{h}_{net,c} + \dot{h}_{net,r} \qquad (13)$$

$$\dot{h}_{net,c} = \alpha_c (\theta_g - \theta_m) \quad W/m^2 \qquad (14)$$

$$\dot{h}_{net,r} = \Phi \cdot \varepsilon_m \cdot \varepsilon_f \cdot 5{,}67 \cdot 10^{-8}$$
$$\cdot \left[(\theta_r + 273)^4 - (\theta_m + 273)^4\right] \quad W/m^2 \qquad (15)$$

The analytical heating presented in this study is obtained by using the emissivity and convective coefficient values proposed in standard EN1993-1-2:2005,[9] which are $\varepsilon_m = 0{,}7$, $\varepsilon_f = 1$ and $\alpha_c = 25W/m^2K$.

Results

Thermal model

Thermal FEM simulates heat transfer in PEBs by convection and radiation through the exposed surface inside the furnace, and allows the temperature field of the beam throughout fire exposure. The thermal behaviour of profile and concrete is simu-lated using ANSYS three-dimensional element SOLID70,[12] the profile-concrete contact is simulated with COMBIN39[12] spring element which connects node by node the profile mesh to the concrete one, and the longitudinal reinforcement is simulated using LINK33[12] bar element, as shown in Figure 3a.

The thermal properties of steel, concrete and reinforcement are those indicated in standards EN1993-1-2:2005[9] and EN1992-1-2:2004,[13] while the thermal behaviour of the profile-concrete contact is defined by a heat flow vs temperature curve, adopting a conductance value of 67W/m²K obtained through the optimization procedure set out in the research conducted by Piloto et al.[14]

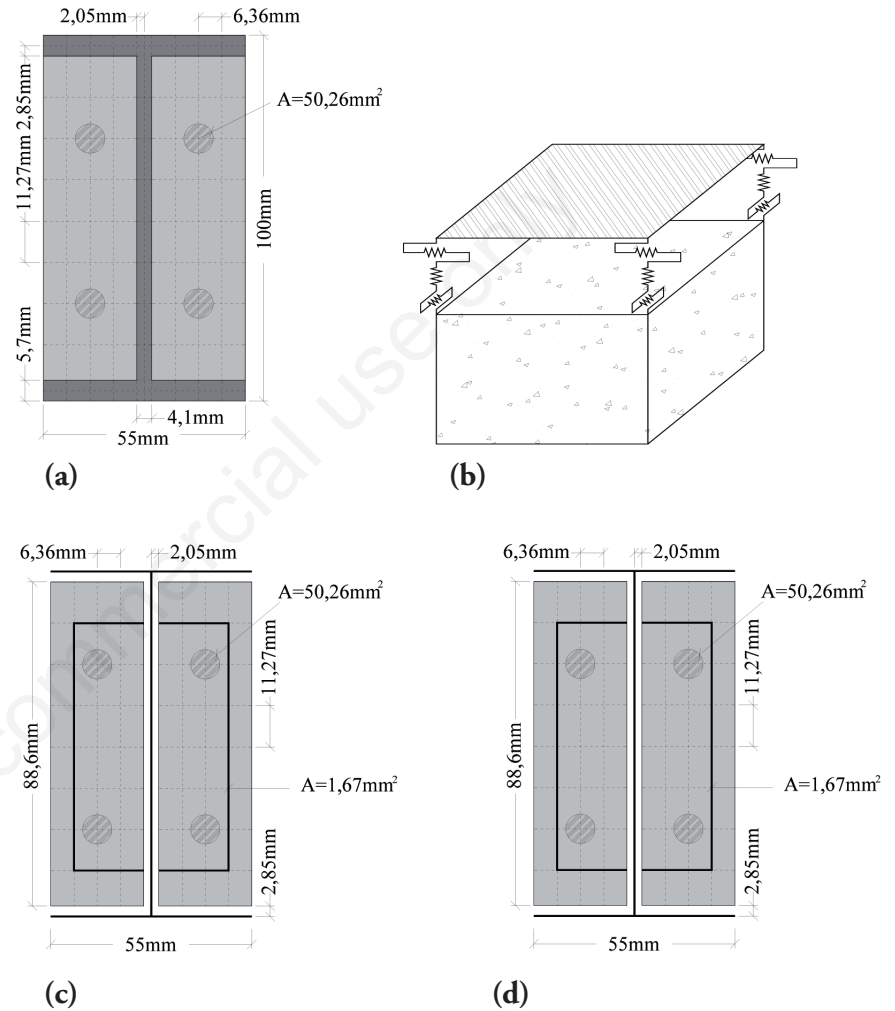Variable fire emissivity and convection coefficients as employed by Wang[15] plus

Figure 3. Numerical model for the analysis of PEBs: (a) Thermal, (b) mechanical; (c) concrete-profile mechanical connection model; (d) modelling of flange-web curve in mechanical model.

Table 1. Section factor of the steel components of the partially encased beam.

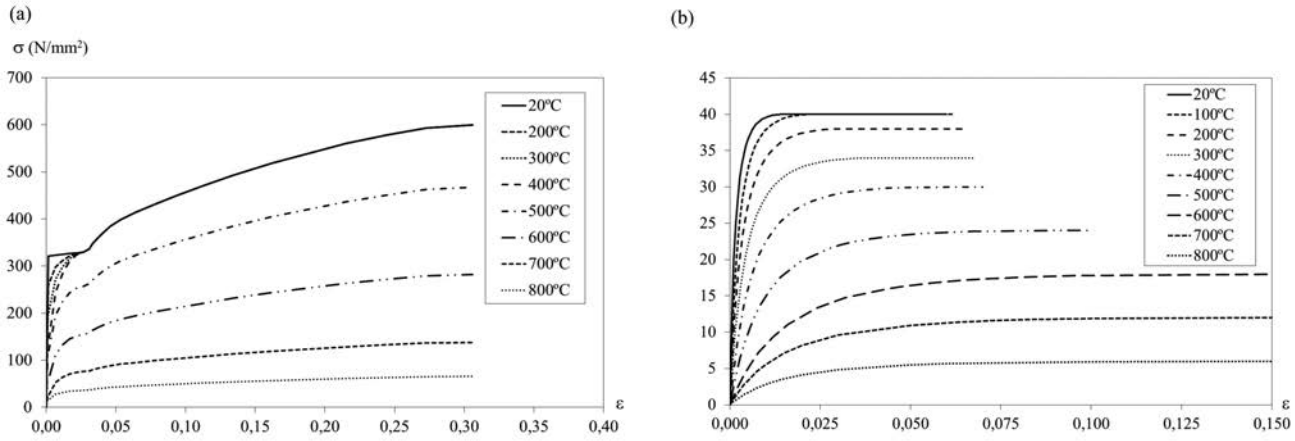| Section factor	Profile flange (a)	Profile web (a)	Profile (b)
$\dfrac{A_i}{V_i} \Big/ \dfrac{A_{p,i}}{V_i}$	$\dfrac{2 \cdot t_f + b}{t_f \cdot b}$	$\dfrac{2}{t_w}$	$\dfrac{2 \cdot (b + 2 \cdot t_f)}{A_{profile}}$

Figure 4. Stress-strain curves used in the numerical analysis of (a) the steel of the profile and (b) the concrete, at different temperature levels.

0.88 and 0.7 emissivity values for steel and concrete are used to validate the numerical model against the fire performed tests.[4,16] However, the numerical study of instability for different load level under fire conditions assumes a constant total emissivity value of 0.7 and a convection coefficient of $25W/m^2K$ on steel and concrete exposed surfaces,[8,9].

A multiple load steps is defined by the ANSYS *Array Parameter Method*,[12] that involves the solve command after each load step, that correspond to 10s in ISO834 curve.[5] Newton-Raphson approach is employed to solve nonlinearities, considering convergence criteria based on heat flow rates, with a tolerance value of 0.001.

Mechanical model

The mechanical behaviour of the profile is simulated by using ANSYS shell elements SHELL181[12] placed on the mid-plane of the profile, whose thickness coincides with the nominal one of the flanges and web of IPE100 profiles, as shown in Figure 3b. The reinforced concrete model is discrete, by using solid elements capable of cracking in tension and crushing in compression for the concrete, ANSYS SOLID65,[12] bar elements LINK8[12] for the reinforcement, and assuming perfect contact between them. The section of the longitudinal reinforcement is equal to its nominal area, while the section of the transversal bars, which appear on all sections of the model, matches the ratio between the area and the distance between the stirrups placed in the beam. Based on the model developed by Queiroz *et al.*,[17] the contact between the profile and the concrete is modelled using node-to-node connection through the use of three non-linear spring elements COMBIN39[12] defined by force-displacement curves. Two springs simulate shear contact
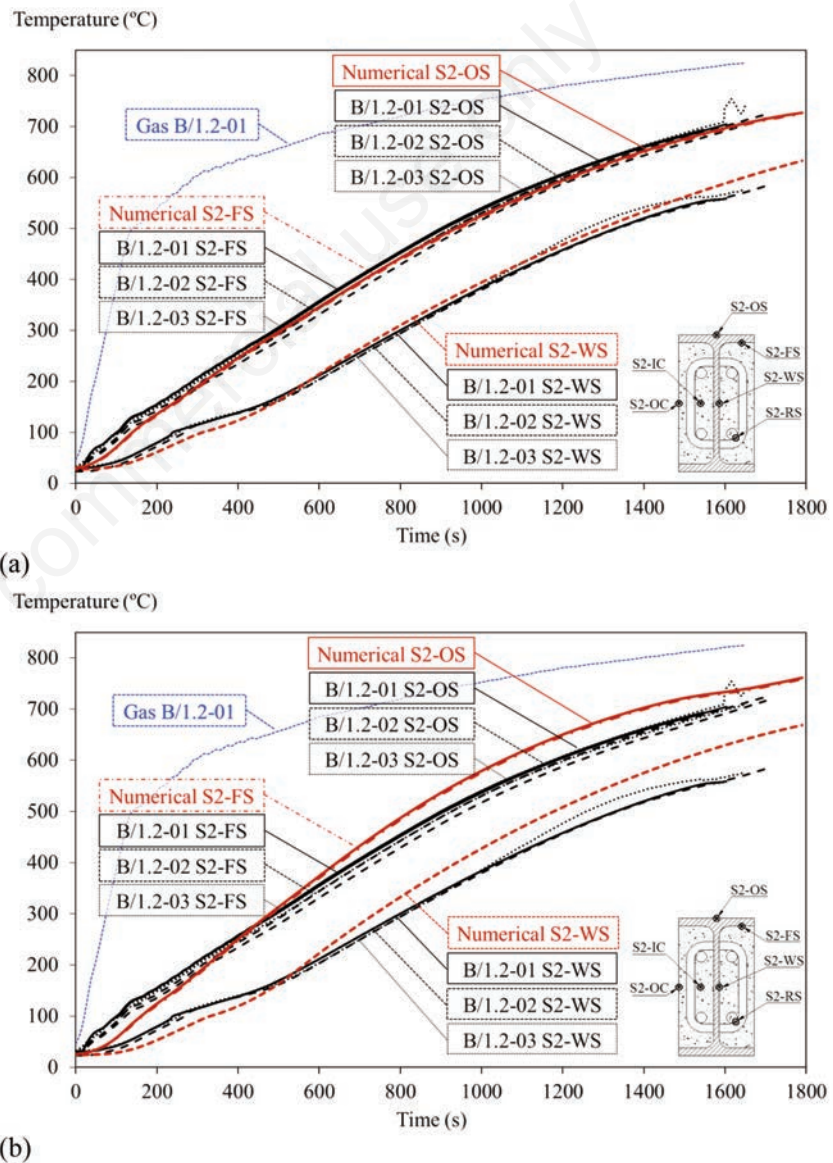

Figure 5. Comparison between numerical and experimental heating of steel profile in load section. a) Variable emissivity and convection coefficients. b) Constant emissivity and convection coefficients.

and the third restricts normal uplifts and compenetrations, as shown in Figure 3c. Shear contact curves simulate adhesion and adherence based in shear bond strength test in PEBs,[18] and normal curves are defined by the slope that allows to simulate the LTB of a 3.9m length PEB experimentally analysed.[16] Tables 2 and 3 show the contact curves per unit bond area. Finally, beam elements BEAM188[12] are introduced into the node indicated in Figure 3d to compensate for curvature and flange-web overlapping.

The stress-strain curve for the steel at room temperature is in line with that obtained from characterization tests,[4] which transforms at elevated temperatures according to EN1993-1-2:2005,[9] as shown in Figure 4a. The stress-strain curve for the concrete at room temperature is in line with that of C20/25 concrete, with a degree of confinement that equals 2, transforming the curve suggested in standard EN1992-1-1:2004[19] applying Mander's model.[20] For different temperature levels, the curves are modified using factors $f_{c,\theta}$, f_{ck}, $\varepsilon_{c1,\theta}$ and $\varepsilon_{cu1,\theta}$ from standard EN1992-1-2:2004,[13] as shown in Figure 4b.

The bottom support, built with a shaft inserted into drilled web, is simulated by blocking the movements of the nodes located on the axis, and the top forked support by cancelling the normal movements along the contour of the nodes that define the forked support. The mechanical load, whose value is constant throughout the thermal loading process, is applied on the common node between the web and the loaded flange at the two mid-span sections, as a percentage of the plastic moment at room temperature, analytically determined in the experimental study[4] based in EN1994-1-1:2004.[6] The numerical study analyses a load level of 20, 37, 41, 56, 61, 74, 82 and 102%, with no lateral restrain. The heating process is simulated by applying the numerical result of the temperature field to each fire exposure time. Multiple load steps are defined with mechanical loads and node temperatures.
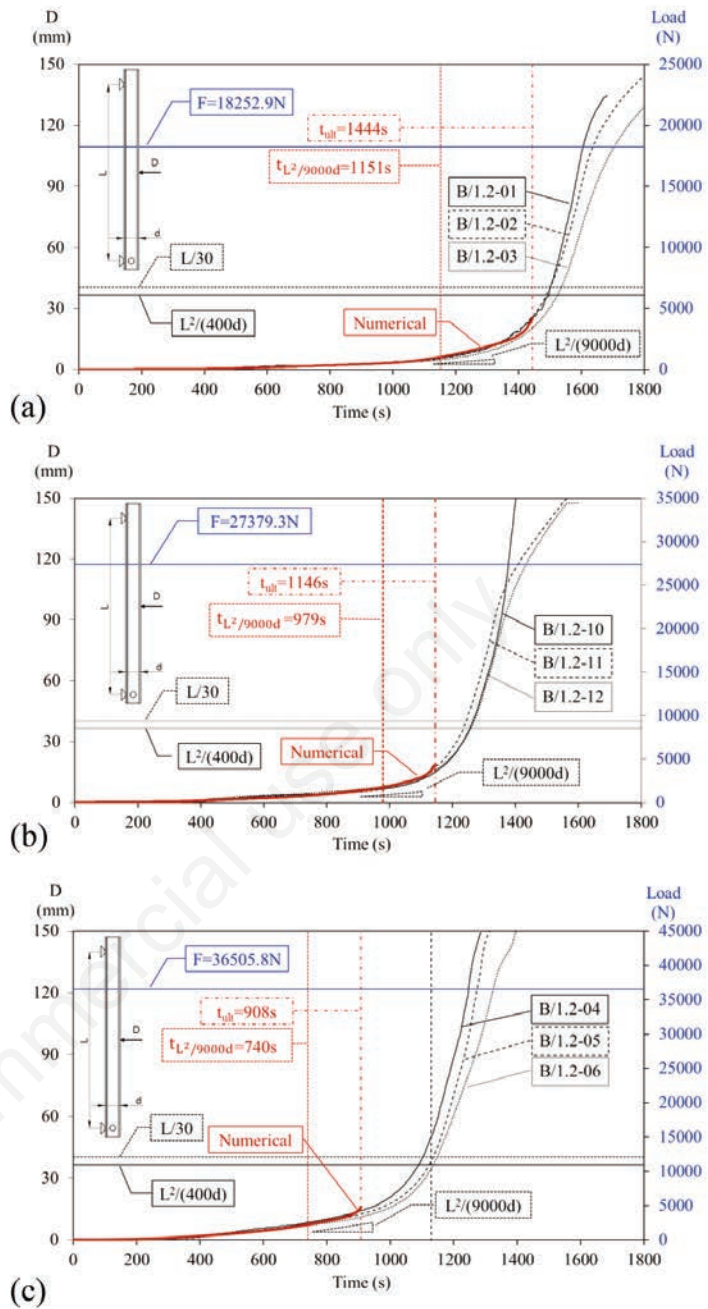

Figure 6. Comparison between numerical and experimental mid-span section deflection under fire. (a) F=40%Mpl, (b) F=60%Mpl, (c) F=80%Mpl.

Table 2. Shear contact load-displacement curves per unit bond area.

Temp. (ºC)						
	Unit of measurement	P1	P2	P3	P4	P5
20	D (m)	0.0	1.0E-8	1.0E-4	5.0E-4	0.1
	F (N/mm²)	0.0	0.118	0.423	0.256	0.079
200	D (m)	0.0	1.0E-8	2.0E-3	5.0E-3	0.1
	F (N/mm²)	0.0	0.115	0.402	0.074	0.073
400	D (m)	0.0	1.0E-8	1.0E-4	5.0E-4	0.1
	F (N/mm²)	0.0	0.102	0.357	0.058	0.057
600	D (m)	0.0	1.0E-8	2.0E-3	5.0E-3	0.1
	F (N/mm²)	0.0	0.079	0.280	0.035	0.034

D, displacement; F, load per unit bond area; P1, 1st point of the curve; P2, 2nd point of the curve; P3, 3rd point of the curve; P4, 4th point of the curve; P5, 5th point of the curve.

Table 3. Normal contact load-displacement curves per unit bond area.

Temp.(ºC)	Load-displacement curve		
		P1	P2
20	D (m)	0.0	1.0E-4
	F (N/mm²)	0.0	102.5
200	D (m)	0.0	1.0E-4
	F (N)	0.0	100
400	D (m)	0.0	1.0E-4
	F (N)	0.0	87.5
600	D (m)	0.0	1.0E-4
	F (N)	0.0	46.25

D, displacement; F, load per unit bond area; P1, 1st point of the curve; P2, 2nd point of the curve.

Newton-Raphson approach is employed to solve nonlinearities, considering convergence criteria based on displacements, with a tolerance value of 0.05.

Model validation

As revealed in Figure 5a, the numerical result obtained with the thermal model that uses variable values of fire emissivity and convection coefficients has the same heating curve in the mid-span section than experimental. The numerical result with constant emissivity and convection coefficients, shown in Figure 5b, gets higher temperature level in all the section points at the heating end.

Applying the first thermal result, the mechanical model correctly simulates the displacements experimentally registered along fire exposure in the upper section and in the load section until the numerical ultimate time, Figures 6 and 7, when lateral instability occurs. As shown Figure 8, numerical lateral displacement results achieve the asymptote, partially restrained in the experimental study.[4] Numerical fire resistance according to standard EN1363-1:2012[10] is reached when the rate of deflection criterion is exceeded, with similar results than experimental.

Numerical deflection results at room temperature have the same evolution than experimentally registered until the numerical final load. The numerical model suffers instability when a 63 kN load is applied while plastic hinge is reached in central sections for a 55.8 kN load, as shown in Figure 9.

Numerical results

Figure 10 shows the numerical displacement results on the mid-span section for different load levels under fire exposure, applying the numerical thermal result of the model that considers the constant emissivity and convection coefficients proposed in standards EN1993-1-2:2005[9] and EN1994-1-2:2005.[8] Numerical ultimate exposure time, when asymptote is reached, and FR according to standard EN1363-1:2012,[10] applying deflection and deflection rate criterion, are resumed in Table 4.

As at room temperature, the numerical result of lateral displacement in the most loaded models does not reach the lateral displacement asymptote. Newton-Raphson approach presents solve difficulties in LTB simulation especially once reached plastic hinge in central sections, even though the numerical model obtains the instant of instability onset.
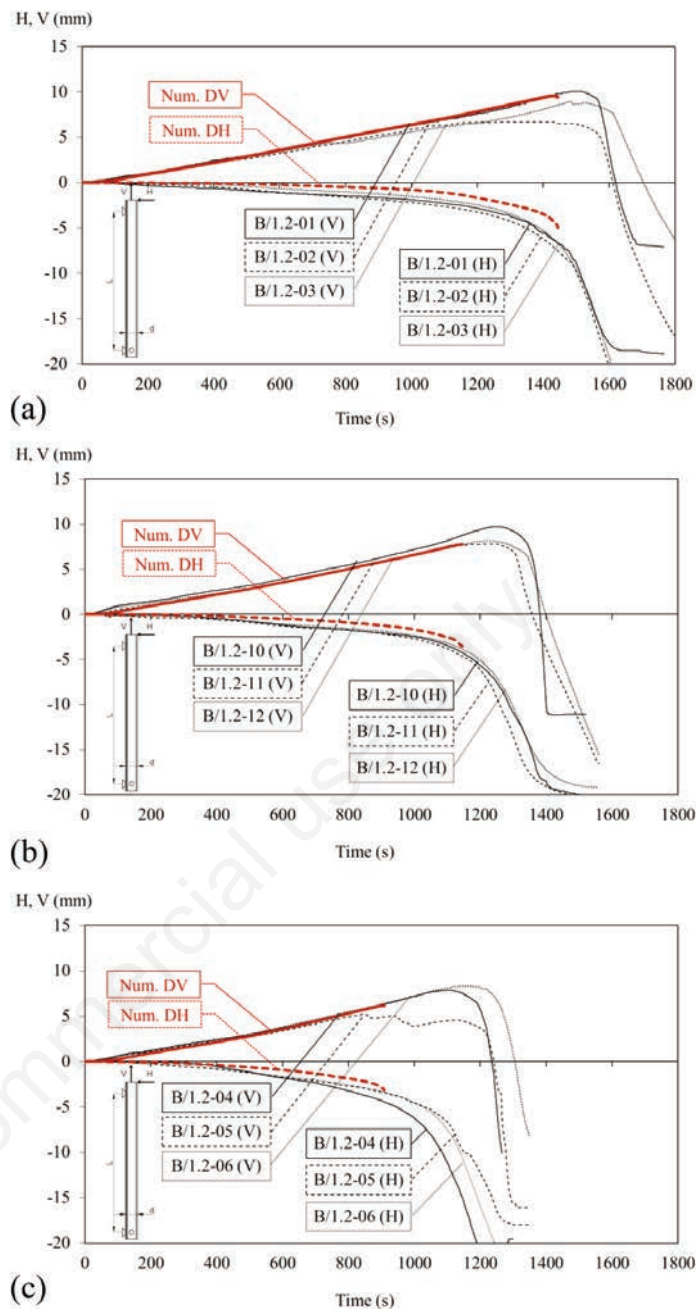
Figure 7. Comparison between numerical and experimental displacement in upper section under fire. (a) F=40%Mpl, (b) F=60%Mpl, (c) F=80%Mpl.

Table 4. Result of the numerical study of the fire resistance of 1.21 m partially encased beams subjected to three-point bending with different applied load values under standard fire exposure.

Force applied (N)	Load level (% Mpl)	t_{ult} (s)	$t_{EN\ 1363-1}$ (s)
10,000	20	1799	1419
18,252	37	1240	988
20,000	41	1203	950
27,379.3	56	990	841
30,000	61	945	809
36,505.9	74	810	638
40,000	82	721.9	588
50,000	102	503	266

t_{ult}, ultimate exposure time; t_{EN}, fire resistance based in standard EN 1363-1:2012.

Discussion

In this section analytical results are compared with numerical and experimental to assess the proposed calculation method.

Figure 11 shows analytical results of buckling resistance moment under fire at time t based on experimental temperature measurements,[4] considering 10 and 100% of the torsional stiffness of the complete encasement. In both cases two uniform temperatures are considered in the steel profile: experimental average temperature,[4] $\theta_s{}^{s2}$, and experimental maximum temperature, $\theta_{a,com}$. Additionally, the moment resistance of the homogenised section in the fire condition determined by EN1994-1-2:2005[8] considering the experimental[4] average temperature is represented. Analytical results are compared with experimental and numerical outlined in point 3.3, using variable fire emissivity and convection coefficients. Curves that consider 100% of the torsional stiffness of the complete encasement have good agreement. Numerical and experimental fire resistance according to standard EN1363-1:2012[10] adjust to analytical considering the maximum steel profile temperature, while numerical instability under fire fits better with analytical considering the average steel profile temperature. The moment resistance of the homogenised section in the fire condition at time t overestimate the fire resistance of PEBs in all analysed load levels.

Figure 12 shows the analytical result of the temperature evolution of the profile assuming uniform temperature in the section. The analytical curve is consistent with the numerical results for the temperature evolution in the flange, overvaluing the average steel profile temperature. Based on this analytical temperature result, Figure 13 shows the analytical result for moment resistance on uniform temperature, $M_{fi,\theta,Rd}$, and for buckling resistance moment on uniform temperature, $M_{b,fi,\theta,Rd}$. These curves are compared with the numerical results obtained with the finite element model that employs constant fire emissivity and convection coefficients proposed in standards EN1993-1-2:2005[9] and EN1994-1-2:2005,[8] set out in section 3.4. Analytical buckling resistance moment curve is consistent with the numerical FR according to standard EN1363-1:2012,[4] but underestimates the ultimate instant when the model attains LTB.

For steel beams, standard EN1993-1-2:2005[9] establishes that the buckling moment resistance at time t is obtained modifying the moment resistance on uniform temperature, $M_{fi,\theta,Rd}$, by the non-uniform temperature across the section factor,
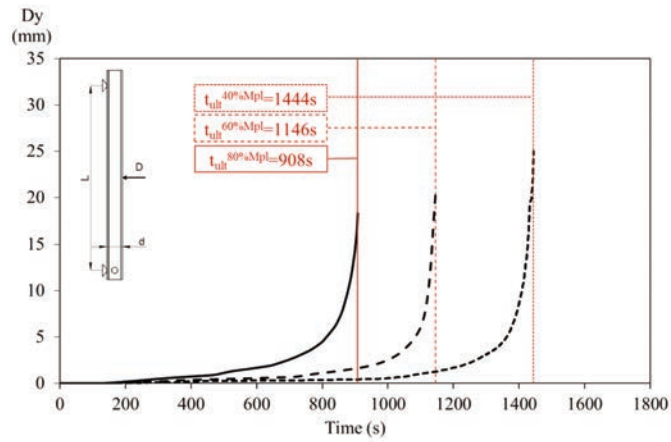

Figure 8. Numerical mid-span section lateral displacement in models that simulate experimental tests under fire.
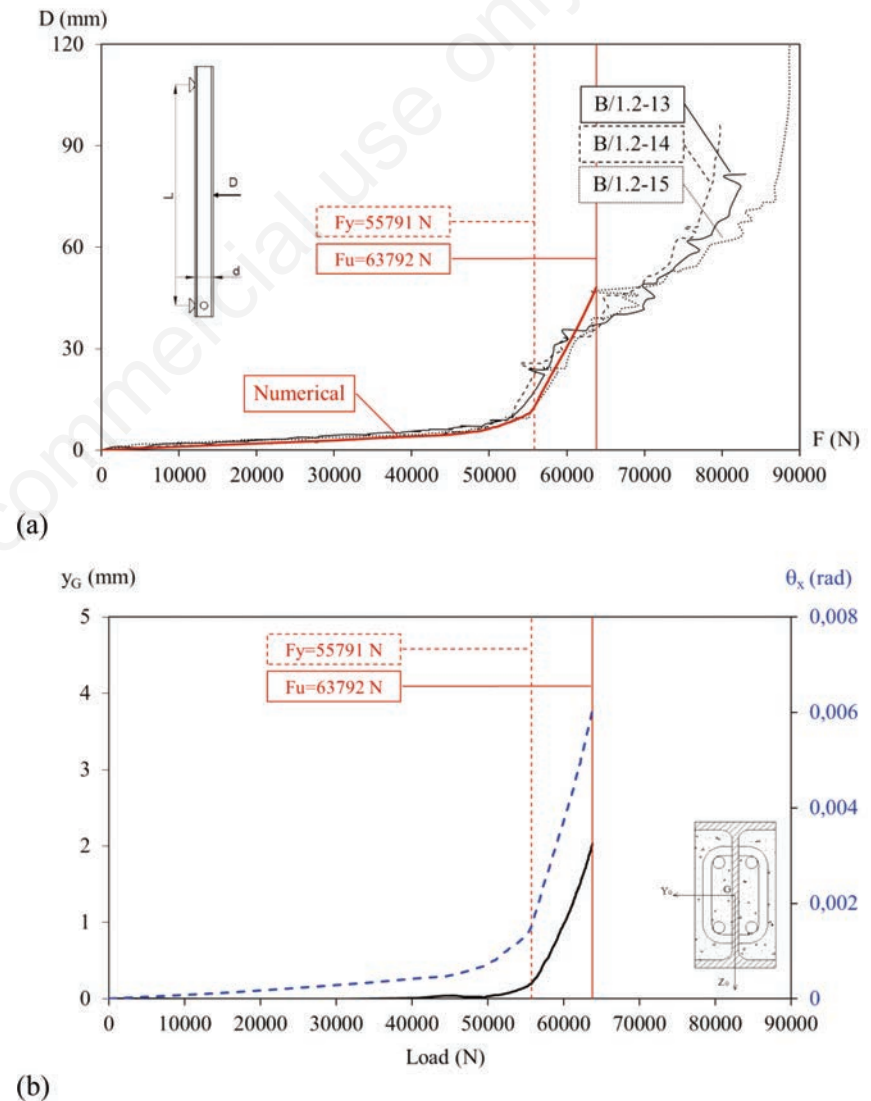

(a)

(b)

Figure 9. Numerical mid-span section displacement at room temperature. (a) Comparison between numerical and experimental deflection. (b) Lateral displacement and axial rotation.

k1, and non-uniform temperature along the beam factor, k2, as exposed in expression (16). Applying this method to PEBs, analytical buckling moment resistance at time *t* improves adjustment to the ultimate numerical instant. Figure 13 shows the analytical results obtained adopting the minor *k1* value proposed in standard EN1993-1-2:2005,[9] 0.7, and the maximum value for *k2*, 1, as analysed PEBs has a uniform heating along the beam and non-uniform temperature in the section.

$$M_{fi,t,Rd} = M_{fi,\theta,Rd} / k_1 \cdot k_2 \qquad (16)$$

Conclusions

Two finite element models are performed to simulate the thermal and mechanical behaviour of the PEBs experimentally investigated under fire by Piloto *et al*.[4]

Numerical thermal results employing constant emissivity and convection coefficients proposed in standards EN1993-1-2:2005[9] and EN1994-1-2:2005[8] gets higher temperature level than experimentally obtained. However variable fire emissivity and convection coefficients as employed by Wang[15] allow simulating the thermal behaviour of PEBs under fire.[4]

Mechanical model correctly simulates the displacements experimentally registered along fire exposure,[4] but suffer LTB previous than in the experimental study[4] because no lateral restrain is applied in the mid-span section. Nevertheless, numerical fire resistance according to standard EN1363-1:2012[10] is reached with similar results than experimental.

A new proposal method to determine the buckling resistance moment of a laterally unrestrained PEBs under fire at time *t* is proposed, adapting the formulation of standard EN1993-1-2:2005[9] to composite sections.

The analytical buckling resistance moment curve obtained with the proposed method adjusts to the instability results of the numerical model that simulates the experimental tests. For its calculation, experimental heating is employed, a uniform steel temperature equal to the average registered in the profile is adopted, and the 100% of the concrete torsional stiffness is considered. If steel temperature adopts the maximum steel temperature registered, the analytical buckling resistance curve adjusts to the experimental and numerical instants in which the rate of deflection criteria according to standard EN1363-1:2012[10] is reached.
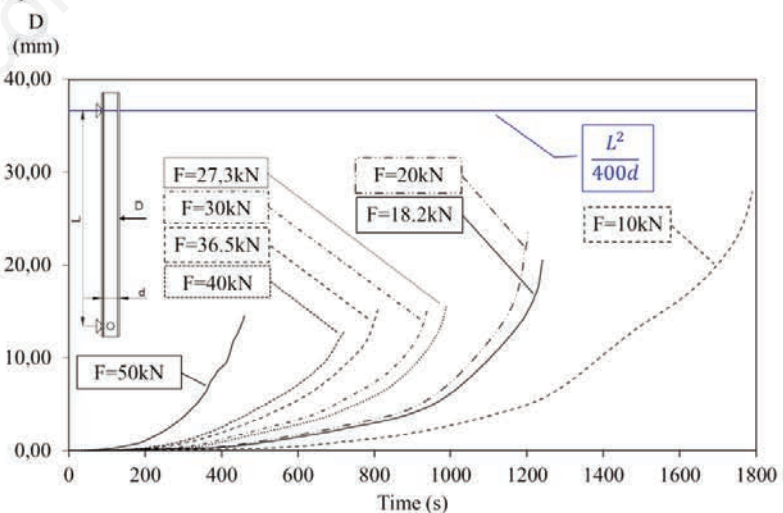
The analytical buckling resistance
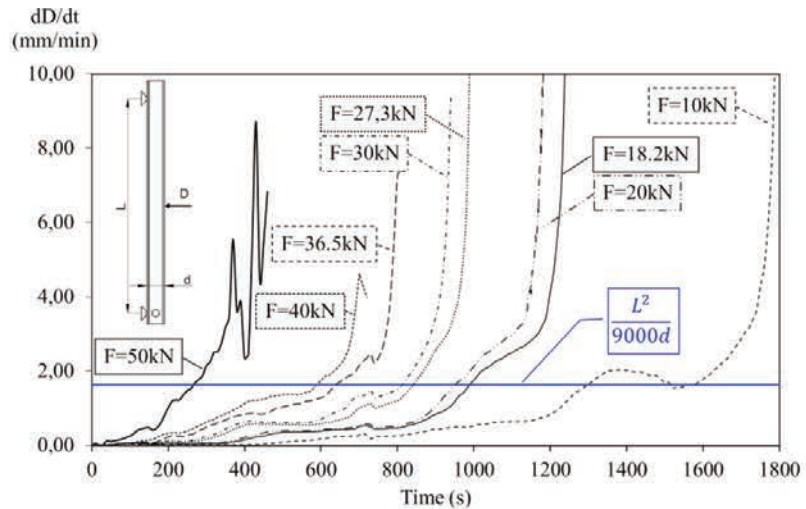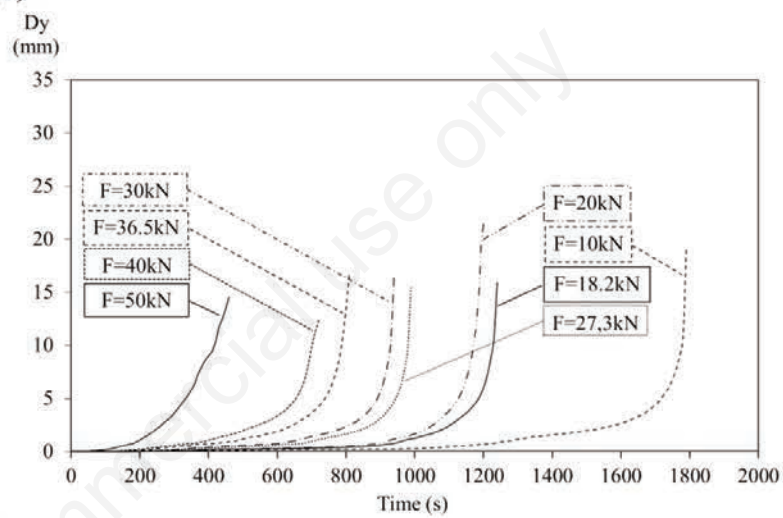
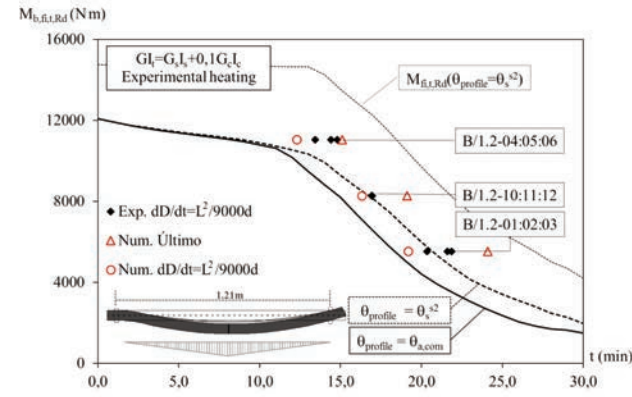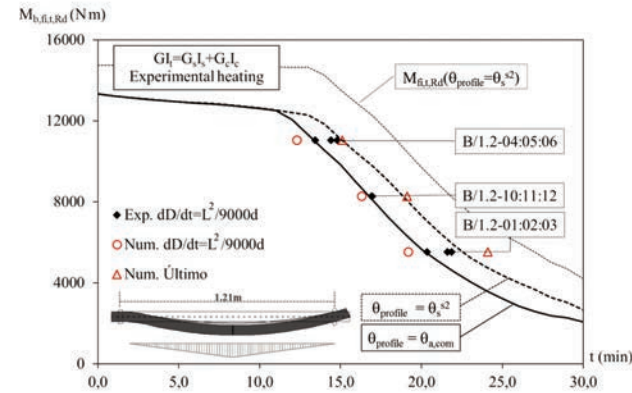**Figure 10. Numerical mid-span section displacement under ISO834 fire exposure considering constant emissivity and convection coefficients. (a) Deflection rate. (b) Lateral displacement. (c) Deflection.**

(a)

(b)

Figure 11. Comparison between analytical results of buckling resistance moment under fire based on experimental temperature measurement and numerical and experimental FR, considering: (a) 10% of concrete torsional stiffness. (b) 100% of concrete torsional stiffness.

Figure 12. Comparison between temperature evolution numerical and analytical results.

Figure 13. Comparison of numerical results simulating standard fire exposure with the analytical results obtained using uniform analytical temperature.

moment curve that considers the uniform analytical heating result according to EN1994-1-2:2005[8] and the 100% of the torsional stiffness, adjusts to the numerical instant in which the rate of deflection criteria according to standard EN1363-1:2012[10] is reached, when numerical model employs the constant emissivity and convection coefficients proposed in standards EN1993-1-2:2005[9] and EN1994-1-2:2005.[8] Applying non-uniform temperature factors, analytical buckling moment resistance at time t improves adjustment to the numerical instability moment.

The numerical model allows validating the proposed calculation method to determine the LTB resistance moment at time t of unrestrained PEBs under fire by using the analytical heating result according to standard EN1994-1-2:2005[8] and non-uniform temperature factors that must be modified with respect to those employed for steel beams.

References

1. Lindner J, Budassis N. Lateral torsional buckling of partially encased composite beams without concrete slab. Composite Construction in Steel and Concrete IV, Conference Proceedings, May 28th to June 2nd, Banff, Alberta, Canada; 2000, p.117-128

2. Maquoi R, Heck C, Ville de Goyet V. Lateral torsional buckling in steel and composite beams. European Commission, Brussels, Belgium.

3. Kodaira A, Fujinaka H, Ohashi H, Nishimura T. Fire resistance of composite beams compose of rolled steel profile concreted between flanges. Fire Sci Tech 2004;23:192-208.

4. Piloto PAG, Gavilán ABR, Zipponi M, et al. Experimental investigation of the fire resistance of partially encased beams. J Constr Steel Res 2013;80:121-37.
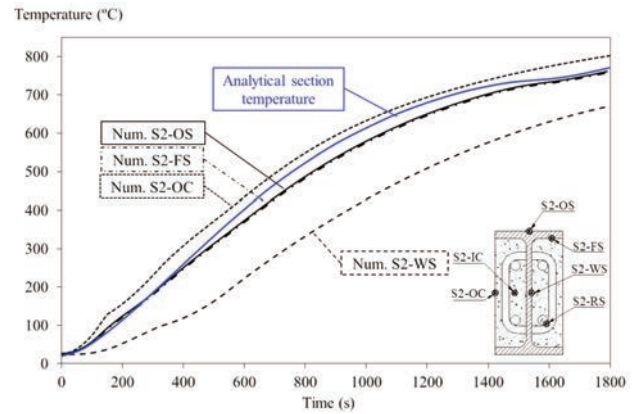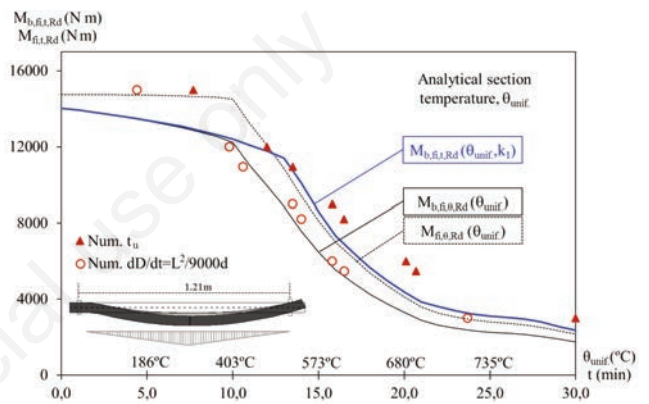
5. ISO 834-1. Fire resistance tests. Elements of building construction. Part 1: General requirements. Geneva: ISO; 1999.

6. CEN - EN 1994-1-1. Eurocode 4: design of composite steel and concrete structures. Part 1-1: General rules and rules for buildings. Brussels: CEN (European Committee for Standardization); 2004.

7. CEN - EN 1993-1-1. Eurocode 3: design of steel structures. Part 1-1: General rules and rules for buildings. Brussels: CEN (European Committee for Standardization); 2005.

8. CEN - EN 1994-1-2. Eurocode 4: design of composite steel and concrete structures. Part 1-2: General rules - Structural fire design. Brussels: CEN (European Committee for Standardization); 2005.

9. CEN - EN 1993-1-2. Eurocode 3: design of steel structures. Part 1-2:

General rules - Structural fire design. Brussels: CEN (European Committee for Standardization); 2005.

10. CEN- EN 1363-1. Fire resistance tests. Part 1: General Requirements. Brussels: CEN (European Committee for Standardization); 2012.

11. Vila Real PMM, Lopes N, Simões da Silva L, Franssen JM. Lateral-torsional buckling of unrestrained steel beams under fire conditions: improvement of EC3 proposal. Comput Struct 2004;82:1737-44.

12. ANSYS® Academic Research. Release 14.0, ANSYS help system. Canonsburg, PA: ANSYS; 2011.

13. CEN - EN 1992-1-2. Eurocode 2: design of concrete structures. Part 1-2: General rules. Structural fire design. Brussels: CEN (European Committee for Standardization); 2004.

14. Piloto PAG, Ramos-Gavilán AB, Mesquita LMR. Determinação numérica da condutância térmica da interface aço-betão para estruturas mistas a temperaturas elevadas. II Conferência Nacional de Métodos Numéricos em Mecânica de Fluidos e Termodinâmica. Aveiro (Portugal), 2008.

15. Wang HB. Heat transfer analysis of components of construction exposed to fire. A theorical, numerical and experimental approach. PhD dissertation. Manchester: University of Salford; 1995.

16. Ramos Gavilán AB. Estudio numérico y experimental del comportamiento a flexión de vigas parcialmente embebidas sometidas a altas temperaturas. PhD dissertation. Salamanca: University of Salamanca; 2015.

17. Queiroz FD, Vellasco PCGS, Nethercot DA. Finite element modelling of composite beams with full and partial shear connection. J Constr Steel Res 2007;63:505-21.

18. Ramos Gavilán AB, Piloto PAG, Mesquita LMR. Estudio del contacto entre el perfil metálico y hormigón en vigas parcialmente embebidas. CMNE/CILAMCE workshop Congresso de Métodos Numéricos em Engenharia. Porto (Portugal), 2007.

19. CEN-EN 1992-1-1. Eurocode 2: design of concrete structures. Part 1-1: general rules and rules for buildings. Brussels: CEN (European Committee for Standardization); 2004.

20. Mander J, Priestley M, Park R. Theoretical stress-strain model for confined concrete. J Struct Eng 1988;114: 1804-6.